AEGC Australasian Exploration Geoscience Conference | Brisbane 2023

UCS while drilling - actionable orebody intelligence for mining efficiency improvement.

R. Griffiths
Orica
roger.griffiths@orica.com

Dr. S. Warden
Orica
sheldon.warden@orica.com

Y. Solovyov
Orica
yuri.solovyov@orica.com

C.Luu
Orica
cu.luu@orica.com

N. Rivadeneyra
Orica
natal.rivadeneyra@orica.com

J. Minto
Orica
james.minto@orica.com

O. Alferez
Orica
oliver.alferez@orica.com

SUMMARY

Uniaxial Compressive Strength (UCS), also known as unconfined compressive strength, is a key rock property which influences multiple steps along the mining value chain including drilling, blasting and comminution operations. UCS is usually measured on drill cores in the laboratory, a process that is both time consuming and expensive, while offering very limited sampling of the overall volume of rock to be extracted. We have developed a novel accelerometer-based measurement acquired while drilling which can determine the UCS of the rock being drilled from the vibrations induced in the drillstring. The fundamental response measured is a time delay, not a force or torque, and so does not suffer from the calibration and consistency issues that plague attempted application of Measurement while drilling (MWD) data to rock parameter determination. In addition, the measurement is insensitive to bit condition and driller actions, resulting in a significantly more robust evaluation of the subsurface than available through MWD analysis. The measured delay correlates strongly with UCS, so when acquired during blasthole drilling the measurement provides high resolution UCS data with fine spatial sampling, providing a rich, statistically-significant dataset for determination of the distribution of rock strength. This information feeds into drilling, blasting and comminution optimization. Drilling through the current bench and sampling the next bench down expands the application of this measurement to drill pattern planning based on the measured mechanical properties of the next bench. Survey hardware, deployment and processing is presented along with an example application to a copper porphyry mine.

Key words: UCS, while drilling, orebody intelligence, blast design, fragmentation.

INTRODUCTION

Measurement-While-Drilling (MWD) techniques collect drilling-related data, some of which provide insight into the drilling process and the rocks being drilled. Within the surface mining industry, these data are used to inform blast design by providing rock properties in individual blastholes (Segui and Higgins, 2002), allowing customization of explosives loading and blast patterns to local rock properties. These Drilling and Blasting (D&B) parameters influence blast fragmentation, reducing crushing and milling costs by optimizing blast comminution efficiency (Ranjbar et al. 2021). Scientometrics database analysis by Isheyskiy and Sanchidrian (2020) reveals significant growth of MWD-related references over the last 20 years, demonstrating increasing industry interest in these methods. Improvement in mine connectivity allows MWD data to be uploaded to the Cloud for processing and analysis. In addition, recent machine learning techniques help improve MWD data correlations to rock properties (Kadkhodaie et al., 2010; Khushaba et al., 2021).

MWD parameters such as Rate of Penetration (ROP), Force-on-String (FOS), Torque-on-String (Torq), and bit Revolutions Per Minute (RPM) which are typically used to monitor drilling operations, can also shed light on the mechanical properties of the subsurface. However, results from this type of analysis have been mixed as the measurements are not always well calibrated and the empirical correlations applied to the data are not universal.

One of the key mechanical properties of interest is Uniaxial Compressive Strength (UCS), which is also referred to as unconstrained compressive strength. UCS is defined as “the maximum compressive stress that can be applied to a material, such as a rock, under given conditions, before failure occurs” (AGI). The given conditions include single-axis compression (hence uniaxial) without perpendicular stress on the sample (hence unconstrained). UCS values typically range from less than 5MPa (very low strength or very weak rocks) to greater than 250MPa (very high strength or extremely strong rocks), as defined by the International Society for Rock Mechanics (ISRM) (Lu, 2015). UCS is

typically measured in the laboratory either by a localized point load test or a larger scale compressive failure test on drilling cores. Core collection and analysis is a time-consuming and expensive process, preventing real-time data analysis and decision making (Gao et al., 2021; Wang et al., 2020). As discussed by Wang et al. (2020) when working with fractured rocks, samples are sometimes impossible to prepare. In addition, the limited number of samples being tested naturally leads to sparse representation of the rock volume to be mined.

Nainggolan et al. (2018) have shown a good correlation between UCS and blast outcomes as a function of powder factor (the ratio of the mass of explosives to the volume of rock being blasted) with higher powder factor required to deliver consistent fragment sizes with increasing UCS. UCS also supports rock classification (Rahman et al., 2021) and is a key parameter in the design of comminution circuit equipment such as crushers and SAG mills (Lu, 2015). Consequently, several authors have attempted to infer UCS from MWD parameters. For example, Li and Itakura (2012) found a proportional relation between UCS and drilling specific energy for drag bits. The UCS values predicted using this analytical model are in good agreement with those measured on rock cores but require carefully calibrated MWD measurements. More recently, Lakshminarayana et al. (2021) analyse how UCS is related to variations in the drill operating parameters monitored at a CNC drilling machine. They develop multiple higher order regression models to predict UCS from parameters such as thrust and torque.

We introduce a novel measurement derived from a vibrational time delay induced by the interaction of the bit with the rock during drilling. As a time-based measurement it eliminates the need for carefully calibrated load measurements such as weight and torque to be able to characterize the subsurface. The sensor consists of accelerometers mounted on the drillstring, from which raw acceleration time series are processed to derive a relative time delay. This time delay is subsequently correlated with independent UCS measurements to derive a transform to UCS. UCS derived in this manner can then be used to predict blast outcomes, as demonstrated with a case study from a copper porphyry mine. Further applications to mill operations, geology models and drilling optimization are also outlined.

RHINO™ MEASUREMENT

The RHINO™ sensor system is mounted on the drillstring and consists of a set of accelerometers, batteries to power operations for up to two weeks, and a radio link to transmit the data to a surface system in the driller's cab where initial processing is performed before upload to the Cloud. In one configuration the sensor system is magnetically mounted with very strong neodymium magnets at the top of the string (Figure 1)

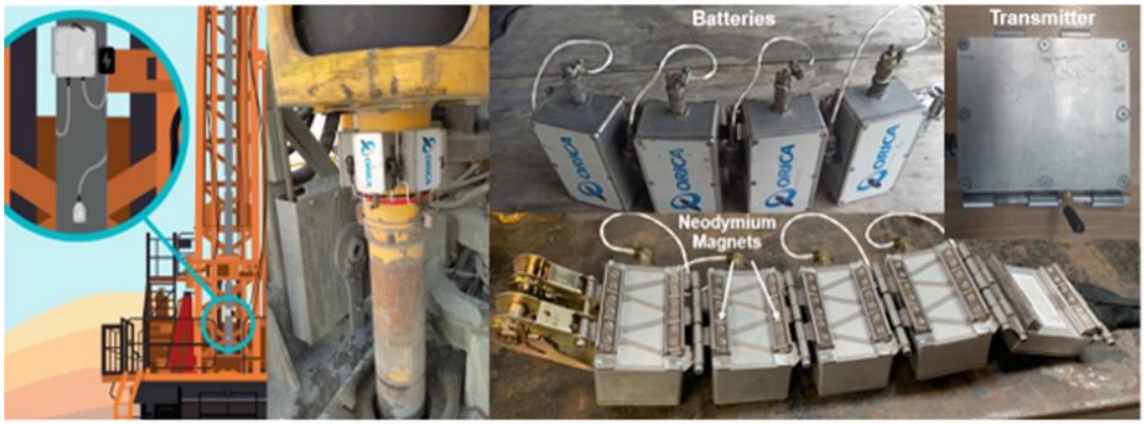

Figure 1. Sensor system deployment. Accelerometers, batteries and radio transmission modules are magnetically mounted at the top of the drillstring.

The system consists of separate radio and battery modules which can be configured to accommodate a wide range of drillstring diameters. Batteries sufficient for two weeks of continuous operation can be fitted on drill strings with a diameter of 7 5/8" or greater. Smaller drill string diameters can be accommodated but with reduced battery capacity and hence increased servicing frequency. The surface acquisition computer is connected to rig power and turns on and off with the drill rig, allowing automatic resumption of acquisition after periods of shutdown.

The radio link, used to transmit both accelerometer and system health data, can be operated across a range of frequencies around 900 MHz to comply with local regulatory or in-pit requirements. System health data such as battery voltages and Received Signal Strength Indicator (RSSI) can be monitored either locally in the driller's cab or remotely, allowing the system to be deployed on both manned and autonomous drill rigs. Data are pre-processed on the surface computer before being uploaded to the Cloud via WiFi or 4G/5G LTE, either through the mine's network or via a third-party provider. Data are also backed up on the surface computer for subsequent manual upload in case of poor in-pit connectivity.

MEASUREMENT PHYSICS

During rotary drilling with a tricone bit, each bit tooth interaction with the rock behaves like a point-load UCS test as the rock is compressed until failure. As the load on the bit tooth increases the rock underneath it initially responds elastically. Obeying Newton's second law, the rock exerts a reactive force equal to the force applied by the bit during this elastic loading phase. But the reactive force is slightly time-delayed relative to the applied force as the rock deforms elastically under the bit tooth load. This delayed reactive force creates an acceleration in the drillstring which is slightly time-delayed relative to the drillstring motion that induced it (Poletto and Miranda, 2004).
Accelerometers on the drillstring measure both the original set of vibrational accelerations in the drillstring and the slightly time-delayed echo of these vibrations associated with drill bit interaction with the rock. Unlike conventional geophysical seismic measurements where the energy travels from a source to a remote receiver, this measurement utilizes the bit as both source and receiver. The near-field effects (Poletto, 2005), which result in the time delay provide a high-resolution measurement as the response occurs in the immediate proximity of the bit.

An example axial acceleration time series acquired during the drilling of a multipass hole is shown in Figure 2. Drilling took approximately 70 minutes with two rod changes at about 36 and 60 minutes after the beginning of drilling operations, as indicated by the solid black vertical lines.

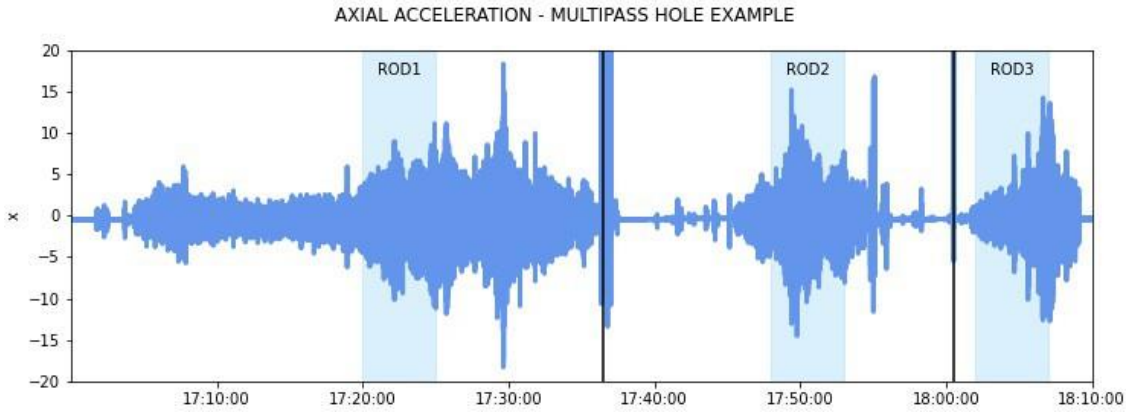

Figure 2. Example axial acceleration time series for a multipass hole. The solid vertical lines indicate the sequential addition of two rods.

The drill string has resonance frequencies at which it naturally tends to vibrate. One of the primary resonances is the axial resonance as compressional waves reflect up and down the drill string. The axial resonance frequency $f_{resonance}$ [Hz] of the system decreases as new rods are added to the drill string due to the increased length that the compressional energy must travel (Figure 3). This frequency is the inverse of the two-way travel time (TWT), where the travel time is equal to the total length of the drillstring $L_{drillstring}$ [m], divided by the group velocity V_{group} [m.s^{-1}]:

$$f_{resonance} = \frac{V_{group}}{2 * L_{drillstring}} \quad (1)$$

The group velocity is given by Carcione and Poletto (2001), where it is computed for the long-wavelength approximation. This expression is consistent with that of Drumheller and Knudsen (1995). The authors provide a formula for N components, which for a simple drillstring comprising a single pipe and a drill collar simplifies to:

$$V_{group} = V_p * \frac{L_{pipe} + L_{collar}}{L_{pipe}^2 + (\frac{A_{pipe}}{A_{collar}} + \frac{A_{collar}}{A_{pipe}}) * L_{pipe} * L_{collar} + L_{collar}^2)} \quad (2)$$

Where V_p [m.s^{-1}] is the compressional velocity in steel, L_{pipe} and L_{collar} [m] the lengths of the pipes and the collar respectively, and A_{pipe} and A_{collar} [m^2] their cross-sectional areas.

To illustrate this concept, Figure 3 displays the power spectral density for the 5 minutes intervals highlighted in light blue in Figure 2, for 1, 2 and 3 identical rods forming a drillstring; the results are shown in Figures 3 (a), (b) and (c) respectively. The dashed black lines indicate the resonance frequencies for group velocities computed using Equation

1. Even though we are using a simple model which does not account for rod thickness variations at connections, the modelled resonance frequencies match the measured frequencies closely, with the resonance frequency decreasing as new rods are added to the drillstring.

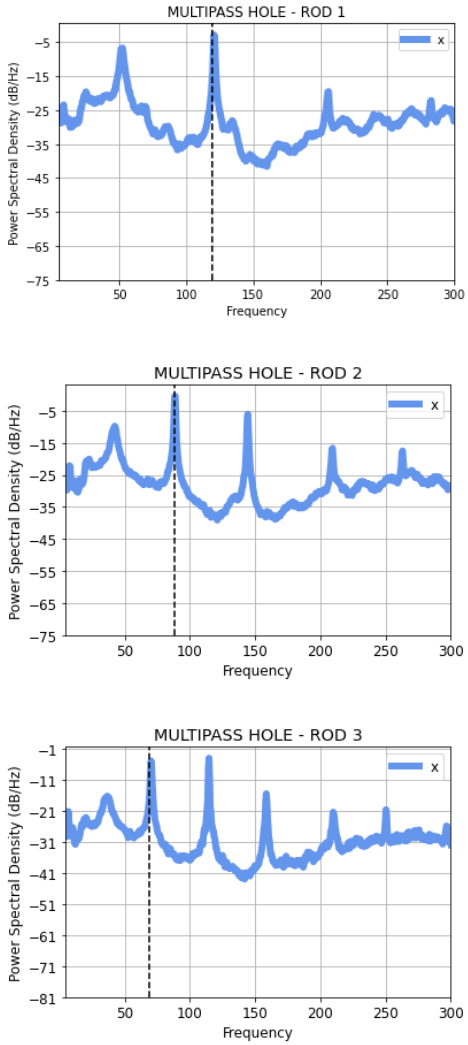

(a) 15.24 m pipe, 4.09 m collar

(b) 22.86 m pipe, 4.09 m collar

(c) 30.48 m pipe, 4.09 m collar

Figure 3. Power density spectra computed over 5-minute windows for (a) 1, (b) 2 and (c) 3 rods. The dashed black lines indicate the axial resonance frequencies computed using equation 1.

Similar analysis can be performed for the torsional, lateral and bending resonance modes of the drillstring. Knowledge of these resonance frequencies is important for the measurement as these constitute the primary vibrational modes propagating up and down the drillstring. These provide the "source signature" on which the time delay is imposed during bit interactions with the rock. Bandpass filtering is applied during processing to ensure that information imprinted on the primary resonance modes is retained while extraneous frequencies are excluded.

MEASUREMENT PROCESSING

One-second drillstring accelerometer traces are autocorrelated and filtered. Autocorrelation provides a relative time reference for the drillpipe acceleration waveform (Poletto and Miranda, 2004). During drilling the acceleration waveform (the vibration) in the drillpipe is continuous. The drillpipe signature reflects up and down the drillstring resulting in constructive and destructive interference with itself. There is no discrete 'source wavelet' as in conventional seismic acquisition. The slightly delayed echo of the drillpipe signature resulting from the bit interaction with the rock is extracted by filtering out the drillpipe signature while accounting for the self-interference effects. Subsequent bandpass filtering and feature extraction is used to determine the time delay.

The time delay data is time-stamped with the UTC clock time at which it was acquired. Bit depth versus UTC time information is required to allow the delay data to be plotted on a depth index. This 1D log of delay versus depth is then correlated with UCS measured on core to derive a delay to UCS transform.

CASE STUDY

Data was acquired on 3 drill rigs at an open-pit copper porphyry mine over a 2-month period in late 2021. Approximately 1900 blastholes were logged delivering over 33 km of data. Hole name, location and drilling depth versus time data was provided by the mine operator allowing the accelerometer data to be converted from a time-index to a depth log, and its spatial position on the bench identified. In addition, geotechnical data such as mineralogy, density, UCS and Rock Quality Designation (RQD) were provided from diamond drilled (DD) core measurements across the mine. RHINO™ accelerometer measurements were acquired in 'twinned' blastholes in the immediate proximity of several of these DD holes to allow correlation of the accelerometer delay response to the core-derived measurements. UCS was measured using the point load method which involves compressing a rock sample between conical steel point load platens until failure occurs. The failure pressure is measured on a pressure gauge and is corrected to yield a point load strength index, which is then converted into a UCS value (Rusnak and Mark, 2000).

Depth adjustment of up to 1 m was required to correlate the measured delays to the core measurements. Depth uncertainties of this magnitude can be readily explained by uncertainty in depth allocation of the core depth such as due to incomplete or disturbed recovered core; discrepancies in elevation measurements of the rig while drilling the DD hole, and/or the rig while drilling the blast hole; uncertainty in the measurement of borehole inclination which results in true vertical depth uncertainty; and timing differences between the clock used to measure depth versus time, and that used to measure rock properties versus time resulting in depth uncertainty in conversion from the time- to depth-index. In addition, the while-drilling data was acquired in 'twin holes' within a meter of the core holes, but formation changes between the holes, particularly in a porphyry geological setting can be significant.

Figure 4 shows a cross plot of the core-derived UCS values against the measured time-delays at the corresponding depth in twin holes drilled close to the diamond drilled core holes. Fitting an exponential function to these data points provides a delay to UCS transform with a high correlation coefficient. For this configuration of the RHINO™ accelerometers in this geological context the transform function was:

$$UCS = 122e^{-2.98\Delta t} \tag{3}$$

where Δt is the RHINO™ delay in ms.

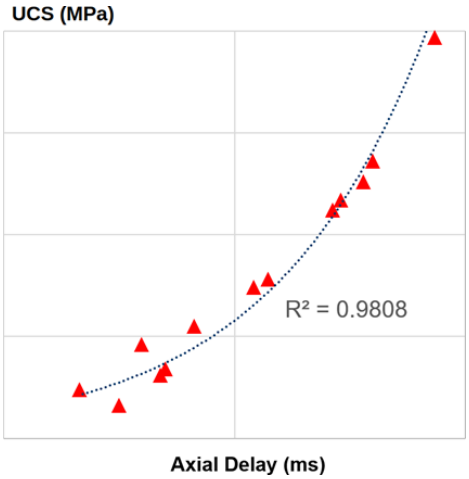

Figure 4. Cross plot of point load UCS measured on core against axial time delay measured on the accelerometers while drilling twinned blast holes in close proximity to the corresponding diamond-drilled core hole. The dotted black line shows an exponential fit with an R^2 correlation coefficient of over 0.98 demonstrating very strong correlation.

The fit is clearly better at high UCS values than at low UCS values. The authors contend that this is a result of the numerous causes that result in soft rock compared to the limited configurations that result in hard rock. For a given mineralogy, the hardest rock will tend to be homogeneous. Fracturing, weathering, porosity or any other source of heterogeneity will tend to weaken the rock. Soft rocks have a variety of mechanisms that can make them soft, not all of which will be captured during a point load test, resulting in more scatter in the point load UCS measurements for softer rocks than for the relatively homogeneous hard rocks.

Applying equation 3 to the continuous time-delay measurement acquired while drilling yields a depth-indexed log of rock UCS, an example of which is shown in Figure 5.

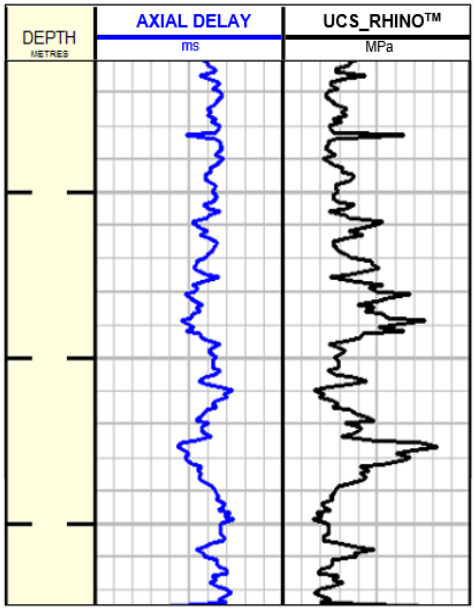

Figure 5. Depth log of measured delay time and rock UCS derived from the delay measurement.

UCS for geology

As numerous blastholes are logged across a bench, a statistically-significant sampling of the rock hardness is acquired. The distribution of rock hardness provides valuable geological information in addition to the absolute hardness of the rock. An example of this additional information is shown in Figure 6 where numerous blastholes are displayed in 3-dimensions. Colour coding shows the UCS values, with blue corresponding to soft rock and red/orange corresponding to hard rock. A fault plane location (brown and blue surface) provided by the operator as part of the geological model is seen to correspond to the soft (blue) rock. This is consistent with fracturing in the proximity of the fault plane resulting in soft rock. The slight misalignment between the fault position indicated by the geological model and the soft rock as measured by the RHINO™ suggests that the geological model can be refined using the measured UCS logs.

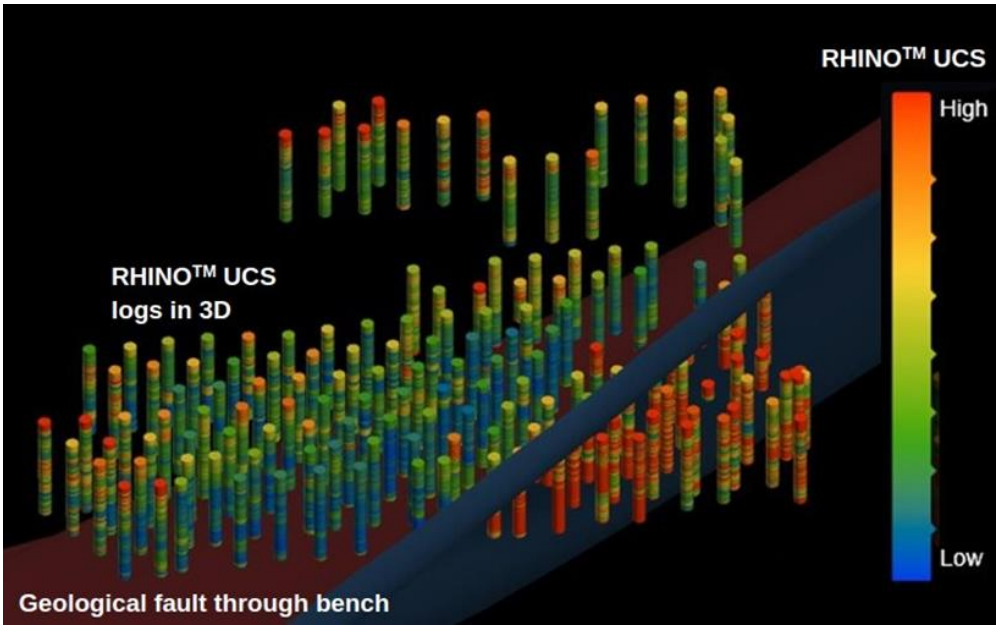

Figure 6. Aggregation of UCS data from multiple blastholes provides additional information. This 3D representation of numerous blastholes across a bench has UCS color-coded along the blastholes with high UCS values in red and orange while low UCS values appear blue and green. The low UCS (blue) interval corresponds to the location of a geological fault (brown and blue surface). The rock in this region is softer due to fracturing associated with movement of the fault. The fault location, provided by the operator before drilling commenced, is several meters further south than suggested by the UCS data. The availability of the array of UCS data allows the geological model to be refined.

UCS for blasting and fragmentation engineering

Where a variety of explosives are used in a single blasthole, knowledge of the UCS distribution along the blasthole allows explosives loading rules to be applied by depth. In cases where only a single explosive type is deployed in each blasthole the lateral variation of rock strength across the bench is required. Leveraging the wealth of UCS data available, a statistical analysis of the UCS distribution can be performed in each blasthole to extract the first (P25), second (median or P50) and third (P75) quartile UCS values. These can be plotted on a map allowing a simplified display of horizontal variation in rock UCS.

Figure 7 shows a colour-coded UCS map across the same drilling pattern as displayed in 3D in Figure 6. Dark colours correspond to low P75 UCS values while light colours correspond to high P75 UCS values. The dark colours correspond to the soft, fractured rock in the proximity of the fault that passes through this drilling pattern. The light colours show the harder, undisturbed rock to the south of the fault.

Figure 7. Horizontal variation in rock UCS value. Plotting a colour-coded map of the third quartile UCS value for each blasthole helps visualize the lateral distribution of rock hardness across a drilling pattern. This example corresponds to the pattern shown in 3D in Figure 6. Dark colours indicate low UCS rock, corresponding to the location of the fault. Lighter colours to the south of the fault indicate harder rock.

Clustering blastholes with similar rock hardness allows blasting domains to be defined. Figure 8 shows the same drill pattern as presented in figure 7 clustered into four rock hardness domains. If similar fragmentation is desired across the pattern, harder zones can be loaded with more or higher-energy explosives while softer zones can be loaded with less or lower-energy explosives.

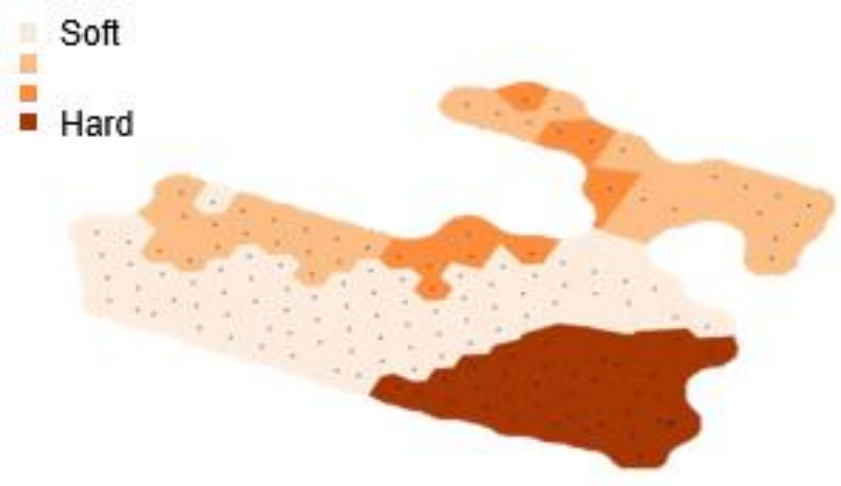

Figure 8. Blasting domains created by clustering blastholes with similar UCS values. In this example four domains have been identified. The number of domains can be adjusted according to the number of different explosive types available.

Blast energy per unit rock mass can be changed either by changing explosive type (energy per unit explosive volume or mass) or by changing the blast hole diameter or drilling pattern (explosive volume per unit rock volume). Blasthole diameter and location cannot be changed after a blasthole has been drilled so planning is required. Drilling through the current bench to sample the UCS distribution in the next bench down allows drill patterns and explosive loading plans to be formulated in advance of operations on the next bench. The detailed UCS distribution of the next bench can then be assessed in detail during blasthole drilling, allowing explosive types and loading rules to be adjusted to optimize rock fragmentation.

In addition to core and geological data, grade block parameters and fragmentation data were made available after blasting of blocks where RHINO™ data had been acquired. A plot of median fragment size against the median UCS measured in the corresponding grade block revealed a strong linear correlation, as shown in Figure 9. This suggests that, for a given powder factor, the median fragment size can be predicted from the median measured UCS.

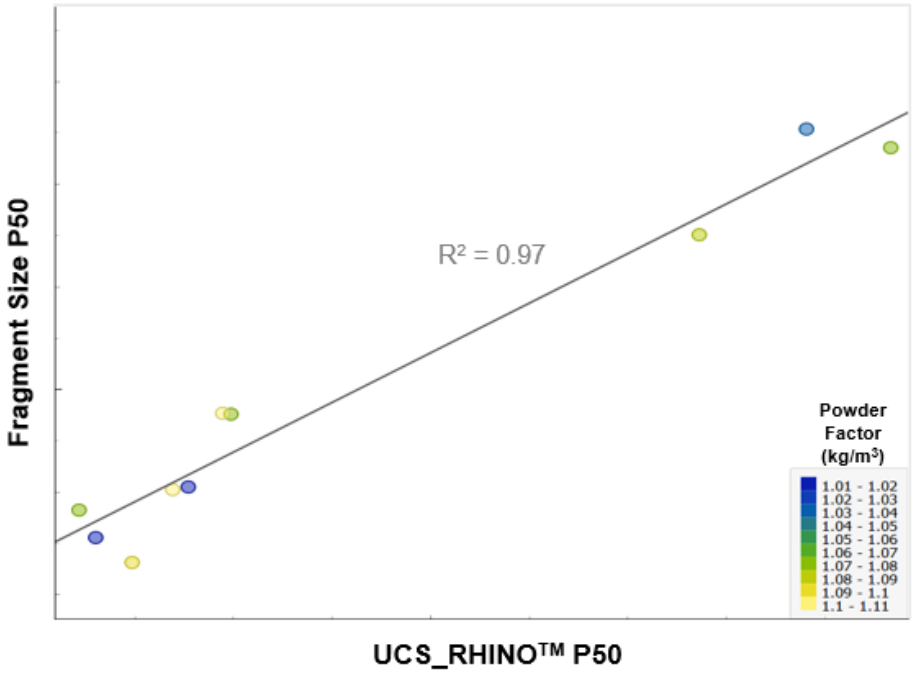

Figure 9. Fragmentation correlation to UCS for a given powder factor, in this case a powder factor of close to 1 kg/m^3. The median fragment size shows a strong linear correlation to the median UCS measured in ten grade blocks that were blasted with similar powder factors.

Similar correlation with blast outcomes was performed on a number of parameters including grade block density, RQD (a rock in-situ fragmentation index), grade block UCS and median drilling rate of penetration (ROP_P50). Table 1 shows the R^2 correlation coefficients between the P20, P50 and P80 fragment sizes (mm) and the percentage of fragments less than 25 mm and 100 mm in size, against these grade block parameters. For this mine, median ROP, density and RQD are poor predictors of blast fragmentation outcome. The assigned grade block UCS is a reasonable indicator despite being sparsely sampled. The excellent correlation between UCS_RHINO™_P50 and blast outcomes appears to be a consequence of this metric capturing rock properties of direct relevance to blast outcomes (UCS) in a statistically meaningful manner by sampling the full grade block in 3-dimensions.

	Density	RQD	Grade Block UCS	ROP_P50	UCS_RHINO™_P50
P20*	0.50	0.65	0.88	0.17	0.96
P50*	0.51	0.68	0.87	0.15	0.97
P80*	0.46	0.76	0.81	0.12	0.95
25mm*	0.44	0.64	0.80	0.12	0.89
100mm*	0.46	0.75	0.79	0.09	0.94

* For grade blocks blasted with Powder Factors of 1 to 1.1 kg/m^3

Table 1. R^2 correlation coefficients between measured parameters (columns) and blast outcomes (rows) for the 10 grade blocks in which the powder factor applied during blasting was between 1 and 1.1 kg/m^3.

UCS for comminution circuit design

Downstream of drill and blast operations, the availability of a statistically meaningful UCS distribution of the mined ore provides opportunities to enhance stockpile management in addition to crusher and mill operations. Drop Weight Index (DWi) is a key parameter in comminution circuit design and optimization, describing the energy per unit volume required to achieve certain fragment size reduction (Morell, 2006).

The DWi has the units of kWh/m3, which has the same dimensionality as hardness (eg MPa) and hence it is not surprising that DWi is correlated with rock strength measurements such as UCS. Figure 10 shows the correlation observed for point load UCS versus DWi from DD core in the case study mine. This clearly demonstrates that UCS is related to parameters of interest for mill performance, opening the possibility of using the measured UCS data for comminution circuit improvement in addition to blasting optimization.

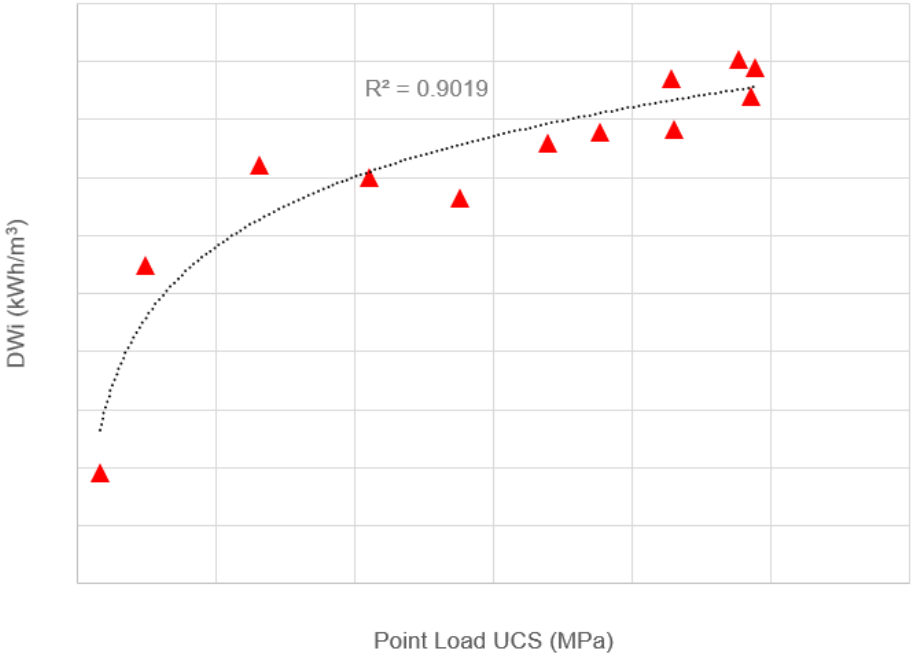

Figure 10. Drop Weight Index versus UCS showing a logarithmic correlation.

UCS for drilling

MWD parameters acquired at surface such as Rate of Penetration (ROP), Force-on-String (FOS), Torque-on-String (Torq), and drillstring Revolutions Per Minute (RPM) are typically used to monitor drilling operations. Attempts continue to be made to use them to shed light on the mechanical properties of the subsurface. However, results from this type of analysis have had mixed success as acquiring all four measurements consistently has proven to be problematic due to reliability issues, and even when they are all acquired one or more of the measurements is often not well calibrated. Further, the correlation of surface drilling related measurements is subject to many assumptions that may not be valid in all cases.

Mechanical Specific Energy (MSE) is a physics-based transform that calculates the mechanical energy input at surface by the drill rig to remove a unit volume of rock from the subsurface. The volume of rock removed per unit time is given by:

$$Vrock = ROP\ X\ Area\ of\ the\ bit \tag{4}$$

The specific energy is then:

$$SE = \frac{Power}{Vrock} \tag{5}$$

The mechanical specific energy provided by a rotary drilling rig is given by:

$$\boldsymbol{MSE} = \frac{\boldsymbol{FOS}\ (N).\boldsymbol{DL}\ (m)}{\boldsymbol{Bit\ area}\ (m^2).\boldsymbol{DL}\ (m)} + \frac{\boldsymbol{2p}\ (\frac{radians}{rev})\ .\boldsymbol{RPM}\ (\frac{rev}{min}).\boldsymbol{Torq}\ (N.m)}{\boldsymbol{ROP}\ \left(\frac{m}{\min}\right).\boldsymbol{Bit\ area}\ (m^2)} \tag{6}$$

Where DL is the distance through which the force-on-string (FOS) moves. Force multiplied by distance through which it moves gives the energy expended. Bit area multiplied by the length of rock removed corresponds to the volume of rock removed. Hence DL is both the distance through which the FOS imparts energy to the rock and the length of rock which fails and is removed. Dimensional analysis shows similar energy per volume units in the second term of the MSE equation. Note that the S.I. units of MSE are N/m^2, also known as Pascals. MSE is generally quoted in MPa. As this is the same unit as rock hardness it has long been assumed that MSE can be used as a proxy for rock hardness.

UCS is measured by applying a load across a known surface area (a compressive stress). This stress results in a compressive strain in the sample (Figure 11, left panel). UCS is the maximum stress the sample can support. In brittle materials such as rocks, the response of the stress-strain curve plot is almost a straight line (elastic behaviour) up to failure (middle panel). Failure generally occurs due to shearing and subsequent fragmentation resulting in permanent lateral expansion and axial compression of the sample (right panel).

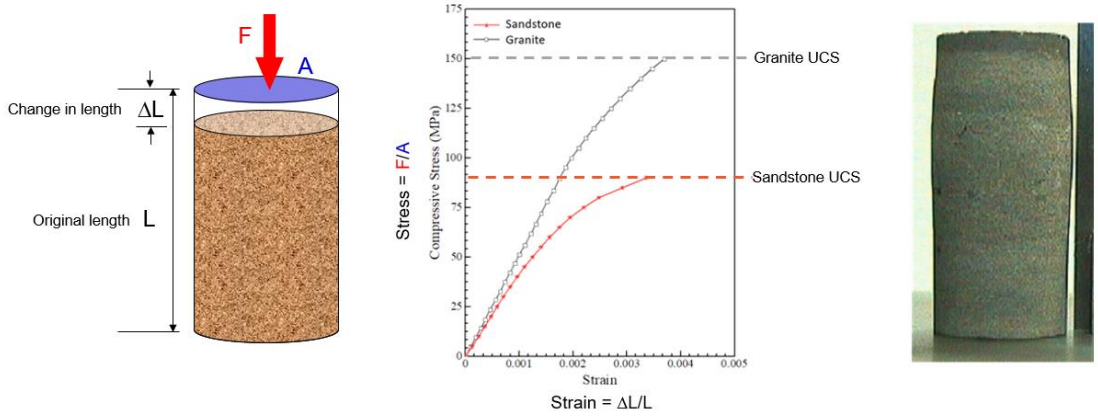

Figure 11. UCS is determined by applying increasing compressive stress on a sample (left panel) until the sample fails and can no longer support the applied load (middle panel). A rock sample after failure due to uniaxial compression (right panel) shows lateral expansion due to movement along shear failure planes and axial compression of the sample.

UCS is the maximum stress at rock failure, and although it has the same units as MSE it is a stress not an energy per unit volume. To quantify the Rock Specific Energy (RSE), the minimum energy required to fail a unit volume of rock, the force must be applied through a distance. As with the first term of the MSE equation, upon failure of the rock the applied force moves through a distance, ΔL, which corresponds to the depth to which the rock fails. So the ratio of the input energy to the volume of rock that fails is given by:

$$\boldsymbol{RSE} = \frac{\boldsymbol{Force\ at\ Rock\ Failure}\ (N)}{\boldsymbol{Area}\ (m^2)}\ x\ \frac{\boldsymbol{DL}\ (m)}{\boldsymbol{DL}\ (m)} \tag{7}$$

The upper product (force x distance = input energy) is the energy required to fail the rock. The lower product (area x length = volume) is the volume of rock that fails. This means that RSE equals UCS as the ΔL terms cancel. Consequently, in a drilling environment rock UCS such as that provided by the RHINO™ accelerometers can be compared to drilling MSE as both provide the energy required to increase hole depth by failing rock at the bottom of the hole. UCS provides the specific energy required to fail the rock itself while MSE provides the entire energy requirement including overcoming friction and other energy losses between the surface and bottom of the hole. Hence, drilling efficiency can be determined by taking the ratio of the rock specific energy and mechanical specific energy:

$$\boldsymbol{Drilling\ Efficiency}\ (\%) = \frac{\boldsymbol{RSE}\ (\frac{MJ}{m^3})}{\boldsymbol{MSE}\ (\frac{MJ}{m^3})}\ x\ 100 = \frac{\boldsymbol{UCS}\ (MPa)}{\boldsymbol{MSE}\ (MPa)}\ x\ 100 \tag{8}$$

Figure 12 compares MWD to RHINO™ data acquired in a hole drilled within 1 m of a core hole so that the UCS values determined from core measurements could be used to create the transform from axial delay measurements to UCS (Equation 3 and Figure 4). The core UCS values (track 3, blue dots) are compared to the corresponding UCS computed from the RHINO™ delays (track 3, red curve).

As has been our experience on most mine sites, the MWD data (track 1) was not complete for this hole (or any of the 1900 holes logged). In this case the RPM data showed zero and then jumped to a value of approximately 10 RPM toward the bottom of the hole (track 1, brown curve). Observations on site suggested that the drillpipe rotation rate was closer to 100 RPM so this value has been applied in calculating the MSE (black curves in tracks 2 and 3). This calculation assumes that the other MWD measurements provided were correctly calibrated.

The RHINO™ axial delay measurement (track 2, blue curve) shows reasonable correlation with MSE, as does the UCS computed from the delay measurement (track 3, red curve). Note that the MSE is slightly increasing with depth while the UCS is trending lower with depth in agreement with the core measured values. This divergence in trends is explained by the drilling efficiency (track 4, green curve) which decreases with depth, suggesting that there is lower efficiency in transfer of energy between the rig and the rock as depth increases.

This underscores the fundamental problem with trying to use MWD data to characterize subsurface rock properties. There is an implicit assumption that the efficiency remains almost constant, but bit wear, borehole friction and an array of other variable energy loss mechanisms calls this assumption into question. By providing UCS, RHINO™ measurements not only allow drilling efficiency to be monitored, but provide a key rock property without the complication of needing to account for energy loss effects. Further, as UCS is acquired using a single sensor, the issues of multiple sensor reliability, calibration and integration are eliminated. This allows a reliable, quantitative, statistically meaningful measurement of subsurface rock hardness to be delivered in a timely manner, facilitating efficiency improvements from the drill to the mill.

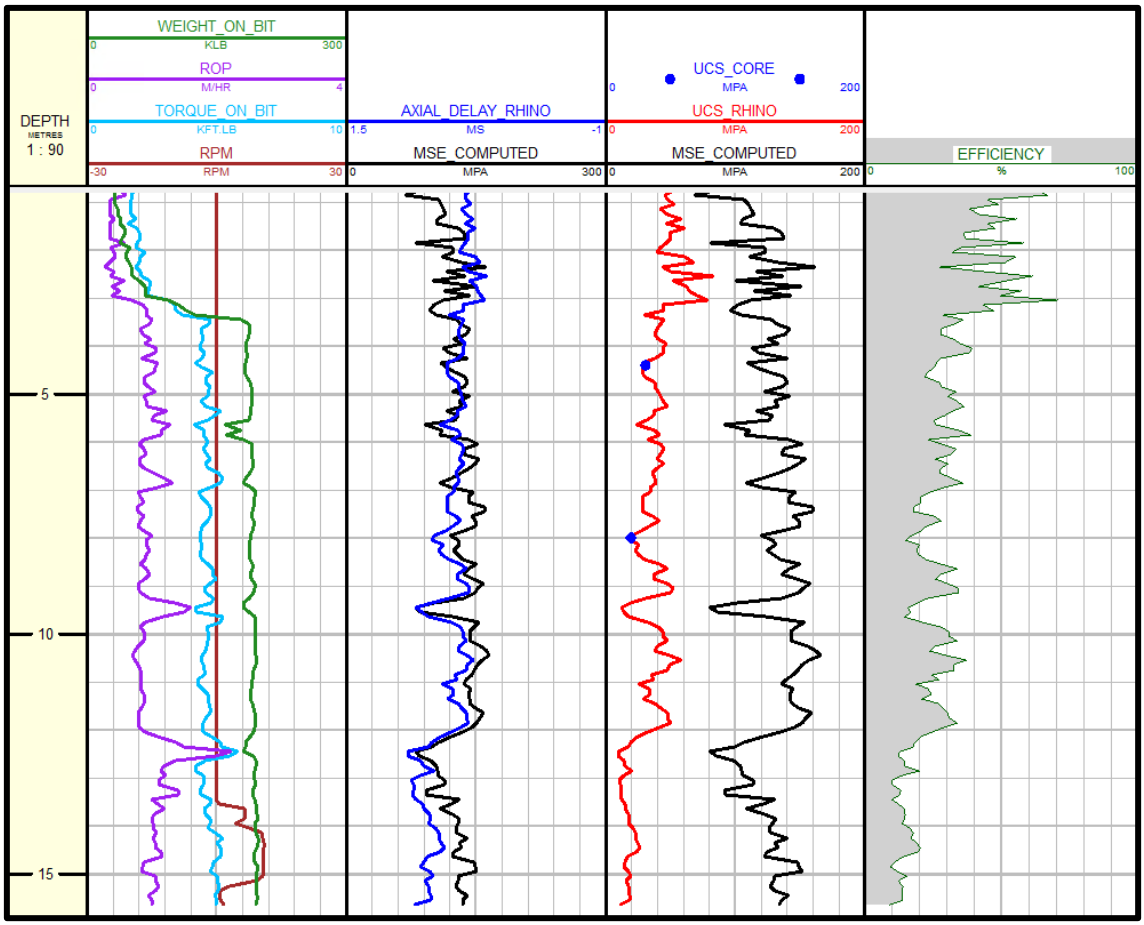

Figure 12. UCS (track 3, red curve) derived from RHINO™ axial delay measurement (track 2, blue curve) correlation to UCS from core samples (track3, blue dots). Strong correlation of both the delay and UCS with MSE (black curve, tracks 2 and 3) is apparent. MSE is computed from MWD data (track 1) despite the typical problem of one of the sensors not working consistently. In this case drillpipe rotation of 100 RPM has been assumed due to a failed RPM sensor. MSE is the energy input by the rig at surface per unit volume of rock removed. UCS is the energy to fail a unit volume of rock. The ratio of UCS/MSE provides the drilling efficiency (track 4), in this case showing decreasing efficiency in energy transfer to the bottom of the hole with depth.

CONCLUSION

A novel accelerometer-derived measurement has been introduced which provides continuous rock UCS data while drilling. When acquired in blastholes across a bench the statistically-significant, spatially-distributed sampling of the rock UCS has been shown to correlate strongly with blast fragment size distribution. This provides the ability to predict blast outcomes and hence optimize explosives loading to deliver engineered fragmentation from blasting. UCS has also been shown to correlate with DWi, a parameter used in mill design and optimization. Further, the ratio of UCS to MSE reveals the efficiency of energy transfer from the drill to the rock, permitting improved drilling performance and highlighting the issues with assuming that MWD data can be used to reliably determine subsurface properties. Hence, UCS measured while drilling provides an opportunity to enhance efficiency at various points along the mine to mill value chain.

ACKNOWLEDGEMENTS

The authors would like to acknowledge the mine operator who permitted their data to be in this paper.

REFERENCES

M. Asgharzadeh, A. Grant, A. B´ona, and M. Urosevic. Drill bit noise imaging without pilot trace, a near-surface interferometry example. Solid Earth, 10:1015–1023, 07 2019. doi: 10.5194/se-10-1015-2019.

J. Carcione and F. Poletto. 2001, On the group velocity of guided waves in drill strings, j. acoust. soc. am., 109(4), 1743-1746. 01 2001.

D. S. Drumheller and S. D. Knudsen. The propagation of sound waves in drill strings. Journal of the Acoustical Society of America; (United States), 4 1995. ISSN 0001-4966. doi: 10.1121/1.412004. URL https://www.osti.gov/biblio/6488559.

A. Egorov, P. Golikov, I. Silvestrov, A. Bakulin, F. Poletto, and B. Farina. Measuring and modeling drillstring vibrations with top drive and near-bit sensors, pages 2749–2753. 2020. doi:10.1190/segam2020-3423747.1. URL https://library.seg.org/doi/abs/10.1190/segam2020-3423747.1.

D. Entwisle, P. Hobbs, L. Jones, D. Gunn, and M. Raines. The relationships between effective porosity, uniaxial compressive strength and sonic velocity of intact borrowdale volcanic group core samples from sellafield. Geotechnical and Geological Engineering, 23:793–809, 11 2005. doi: 10.1007/s10706-004-2143-x.

H. Gao, Q. Wang, B. Jiang, P. Zhang, Z. Jiang, and Y. Wang. Relationship between rock uniaxial compressive strength and digital core drilling parameters and its forecast method. International Journal of Coal Science and Technology, 8, 01 2021. doi: 10.1007/s40789-020-00383-4.

A. B. Haase and R. R. Stewart. Modelling near-field effects in vsp-based q-estimation. art. cp-40-00222, 2008. ISSN 2214-4609. doi: https://doi.org/10.3997/2214-4609.20147762. URL https://www.earthdoc.org/content/papers/10.3997/2214-4609.20147762.

V. Isheyskiy and J. A. Sanchidri´an. Prospects of applying MWD Technology for Quality Management of Drilling and Blasting Operations at Mining Enterprises. Minerals, 10(10), 2020. ISSN 2075-163X. doi: 10.3390/min10100925. URL https://www.mdpi.com/2075-163X/10/10/925.

A. Kadkhodaie, S. Monteiro, F. Ramos, and P. Hatherly. Rock recognition from mwd data: A comparative study of boosting, neural networks, and fuzzy logic. Geoscience and Remote Sensing Letters, IEEE, 7:680 – 684, 11 2010. doi: 10.1109/LGRS.2010.2046312.

R. N. Khushaba, A. Melkumyan, and A. J. Hill. A machine learning approach for material type logging and chemical assaying from autonomous measure-while-drilling (mwd) data. Mathematical Geosciences, pages 1 – 31, 2021.

C. Lakshminarayana, A. Tripathi, and S. Pal. Experimental investigation on potential use of drilling parameters to quantify rock strength. International Journal of Geo- Engineering, 12, 12 2021. doi: 10.1186/s40703-021-00152-5.

L. Li, Y. Liu, W. Liu, X. Zhang, J. Chen, D. Jiang, and J. Fan. Crack evolution and failure modes of shale containing a pre-existing fissure under compression. ACS Omega, 6(39):25461–25475, 2021. doi: 10.1021/acsomega.1c03431. URL https://doi.org/10.1021/acsomega.1c03431.

Z. Li and K. Itakura. An analytical drilling model of drag bits for evaluation of rock strength. Soils and Foundations, 52(2):216–227, 2012. ISSN 0038-0806. doi: https://doi.org/10.1016/j.sandf.2012.02.002. URL https://www.sciencedirect.com/science/article/pii/S0038080612000303.

L. Lu. Iron Ore: Mineralogy, Processing and Environmental Sustainability. Elsevier Science, 2015. ISBN 9781782421566. URL https://books.google.fr/books?id=JvkDwgEACAAJ.

S. Morrell, Design of AG/SAG Mill Circuits using the SMC test, SAG 2006

D. Nainggolan, R. Sitorus, O. Eveny, and F. Sariandi. Correlation between uniaxial compressive strength (ucs) and blasting geometry on rock excavation at pt agincourt resources. IOP Conference Series: Earth and Environmental Science, 212:012065, 12 2018. doi: 10.1088/1755-1315/212/1/012065.

F. Poletto. Energy balance of a drill-bit seismic source, part 1: Rotary energy and radiation properties. GEOPHYSICS, 70(2):T13–T28, 2005. doi: 10.1190/1.1897038. URL https://doi.org/10.1190/1.1897038.

F. Poletto and F. Miranda. Seismic While Drilling: Fundamentals of Drill-Bit Seismic for Exploration. Handbook of Geophysical Exploration: Seismic Exploration. Elsevier Science, 2004. ISBN 9780080474342. URL https://books.google.fr/books?id=HAIZdfDXT2IC.

F. Poletto, F. Miranda, B. Farina, and A. Schleifer. Seismic-while-drilling drill-bit source by ground force: Concept and application. GEOPHYSICS, 85:1–50, 02 2020. doi: 10.1190/geo2019-0449.1.

H. Rafezi and F. Hassani. Drilling signals analysis for tricone bit condition monitoring. International journal of mining science and technology, 31:187–195, 2021.

A. Ranjbar, A. Mousavi, O. Asghari, Using Rock Geomechanical Characteristics to Estimate Bond Work Index for Mining Production Blocks, Mining, Metallurgy & Exploration (2021) 38:2569–2583, https://doi.org/10.1007/s42461-021-00498-5

J. Rusnak and C. Mark. Using the point load test to determine the uniaxial compressive strength of coal measure rock. 01 2000.

J. Segui and M. Higgins. Blast Design Using Measurement While Drilling Parameters. Fragblast, 6(3-4):287–299,2002. doi: 10.1076/frag.6.3.287.14052. URL https://www.tandfonline.com/doi/abs/10.1076/frag.6.3.287.14052.

M. Wang, W. Wan, and Y. Zhao. Prediction of the uniaxial compressive strength of rocks from simple index tests using a random forest predictive model. Comptes Rendus. Mecanique, 348:3–32, 01 2020. doi: 10.5802/crmeca.3.